MICROSTRUCTURAL EVOLUTION IN HIGH TEMPERATURE CREEP AND THERMALLY AGED HA230

J.Veverkova[1], A.Strang[1], G.Marchant[2], G.McColvin[2] and H.V. Atkinson[1]

[1 - Department of Engineering, University Rd., University of Leicester, Leicester, LE1 7RH UK]
[2 - Siemens Industrial Turbomachinery Ltd, Lincoln, UK]

Abstract

Haynes Alloy 230 is a sheet material used for combustor components in a number of small industrial gas turbines manufactured by Siemens. During normal operating service the material is subjected to high temperatures and cyclic mechanical and thermal stresses, which can lead to degradation of the microstructure and mechanical properties of the alloy, and hence limit component design life. As a result of this a long-term programme has been initiated to investigate the effects of thermal and creep exposure on the microstructure of this material using advanced FEGSEM and analytical TEM techniques with the objectives of:

- determining the effects of turbine operating factors on the microstructural evolution of the alloy during service exposure;
- identification of alloy phases which could potentially act as indicators of the average exposure temperatures experienced for specific service periods;
- development of a microstructurally based model to enable the assessment of in-service operating temperatures as an aid to evaluation of the remnant life of HA230 combustor components.

Originally this alloy was specifically designed to have excellent long-term thermal stability and resistance to the precipitation of damaging phases. However, whilst this appears to be true for the case of thermal exposure, there is growing evidence from the studies conducted to date that in addition to M_6C and intergranular precipitation of $M_{23}C_6$ resulting from thermal exposure, other types of phases may also precipitate in the alloy due to time dependent plastic deformation during long-term creep and/or thermo-mechanical fatigue exposure leading to reductions in both ductility and high temperature strength.

This paper describes initial studies on the effects of long-term high temperature exposure on hardness and microstructural changes of creep rupture tested and thermally exposed samples of HA230 being carried out as part of the current COST 538 technology programme..

Keywords - HA230, creep, microstructural evolution, thermal ageing, hardness

Introduction

Haynes Alloy 230™ is a solid solution and carbide strengthened nickel-base superalloy originally developed in the 1980's to meet industry requirements for an alloy with a combination of high temperature strength, long-term thermal stability and outstanding corrosion resistance in oxidising and nitriding environments at service temperatures up to 1150°C. These properties, together with its good formability and weldability characteristics, have made HA230 an ideal material for many aerospace and power industry applications, including the manufacture of gas turbine sheet metal hardware such as combustion cans, transition ducts etc [1].

The alloy was originally developed from the Ni-Cr-Mo-W system in which the high nickel content provides a stable austenitic matrix with tungsten and molybdenum additions, in the presence of carbon and boron, providing the alloy's high temperature strength. Tungsten

provides very effective solid solution strengthening whilst carbon promotes the formation of chromium rich $M_{23}C_6$ carbides. These precipitate on grain and annealing twin boundaries, pinning dislocations and thereby contributing to the alloy's creep strength as well as resistance to grain coarsening during prolonged exposure at high service temperatures. Tungsten was also specifically chosen in preference to molybdenum as a major alloying element, since it diffuses more slowly in nickel. It also increases the elastic modulii and decreases the stacking fault energy, hence impeding cross-slip and promoting high-temperature creep and fatigue strength. Finally resistance to surface attack in oxidising and nitriding environments is provided by the additions of chromium, manganese, silicon and lanthanum, with the latter element contributing to the stabilisation of the surface protective chromia scale during service exposure [2-5].

The wrought product form of the alloy, e.g., bar, plate or sheet, is normally produced by rolling an electro-slag remelted ingot on a reversing mill at a temperature of approximately 1200°C. Thinner gauge sheet products may be finished by cold rolling prior to final annealing. After rolling to the final product size the material is solution annealed within the temperature range 1177 to 1246°C and rapidly cooled or water quenched. This results in an equiaxed microstructure with an average grain size in the range of ASTM 4-6. In this as-received condition, tungsten-rich primary M_6C carbides are present both at grain boundaries and randomly dispersed within the microstructure. These resist resolution during heat treatment thus enabling a grain size range to be achieved which results in the best combination of high temperature creep rupture and LCF properties. In addition to the primary M_6C precipitates present in the annealed condition, some chromium rich $M_{23}C_6$ may also be present precipitated at the grain boundaries and on annealing twins within the microstructure, Figure 1 [2-4].

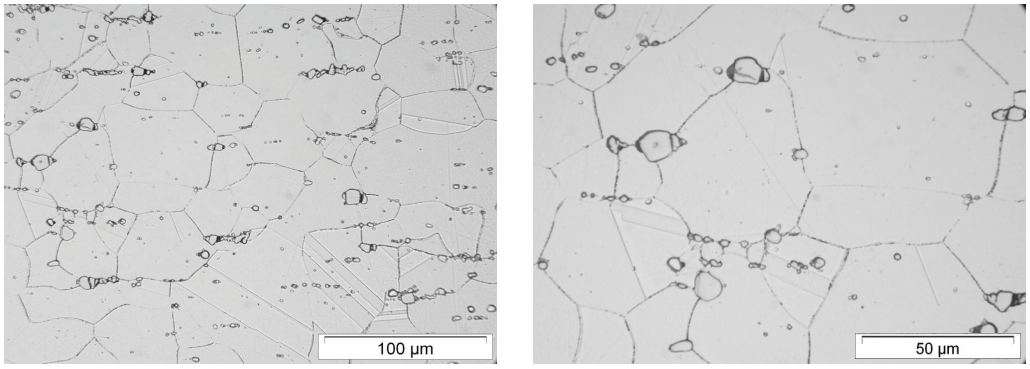

Figure 1 Microstructure of annealed and quenched HA230 showing primary M_6C particles

In industrial gas turbine applications, components such as combustion cans and transition ducts manufactured from the alloy are exposed for prolonged periods of time at high temperatures and experience complex thermal cycles which vary depending on the gas turbine's planned operational and design life requirements. The combined effects of high temperature thermal exposure and accumulated plastic deformation during service cause microstructural changes to occur in the material which significantly affect its mechanical properties and limits the design life expectancy of components manufactured from the material. In practice, these changes can involve precipitation of secondary phases such as carbides and possibly intermetallic compounds, as well as recovery and recrystallisation effects, all of which affect the mechanical properties of the alloy and may impair its fracture resistance. Understanding of these processes and their effects on the thermal and microstructural stability of the alloy is therefore of primary concern, since they may determine the life limiting parameters of combustion hardware design and service performance.

In order to investigate this further, a four year study was undertaken in September 2004 as part of the COST 538 technology programme. The primary thrust of this investigation was to

evaluate the microstructural changes which occur in HA230 in the as-received solution annealed condition when exposed for durations of up to 30,000 hours at temperatures in the range 600°C to 1050°C and compare these with changes observed in material taken from the same heat of this alloy which has been creep rupture tested at temperatures between 600°C to 1000°C for durations of up to 50,000 hours. This paper describes the work carried out in the first phase of the project and includes hardness as well as optical and FEGSEM microscopy studies on thermally exposed and creep tested HA230.

Materials

Both the thermal exposure and creep rupture tests have been carried out on material taken from a single heat of HA230 (No 8305-5-7170) supplied in the form of 2 mm thick sheet in the solution treated and quenched condition by Haynes International Ltd to AMS 5878. Comparisons of the test certificate and AMS5878 specified values for the chemical composition, heat treatment and mechanical properties for this heat are shown in Tables 1 and 2.

Heat	Ni	Cr	W	Mo	Fe	Co	Mn	Si	Al	C	La	B
8305-5-7170	Bal	21.75	13.96	1.32	1.40	0.37	0.49	0.36	0.29	0.12	0.013	0.004
AMS 5878	Bal	20.0 to 24.0	13.00 to 15.00	1.00 to 3.00	3.00 max	5.00 max	0.30 to 1.00	0.25 to 0.75	0.20 to 0.50	0.05 to 0.15	0.005 to 0.05	0.015 max

Table 1 - Chemical Analysis in wt%

Properties	Test Certificate Heat no 8305-5-7170	Specification AMS 5878
Heat Treatment	Solution annealed at 1230°C and quenched	Solution treat between 1177°C and 1246°C and cool rapidly
0.2% Yield Strength	448 MPa	345 MPa min
UTS	859 MPa	793 MPa min
% Elongation	45	40 min
Rupture life at 927°C and 69MPa	50 hrs	36 hrs min
% Elongation	34	10 min
ASTM Grain Size	5.5	3 max

Table 2 Heat Treatment and Mechanical Properties

Results and Discussion

Thermal Exposure Tests

Vickers hardness measurements have been carried out with a load of 20 kg on unstressed coupons of HA230, approximately 30mm x 150 mm in size exposed for up to 15000 hours at temperatures in the range 600°C to 1050°C. The results, which are shown in Figures 2a and b, indicate that systematic changes in hardness occur in the material with increasing exposure durations and temperatures. Initially the hardness increases from an average value of 217.8 Hv20 in the original solution annealed and quenched condition, reaching peak values of 248.3Hv20 and 250.3 Hv20 after exposure for 500 hours and 1000 hours respectively at 650°C, i.e. increases of between 14% and 15% compared with the material in the as-received solution annealed and quenched condition.

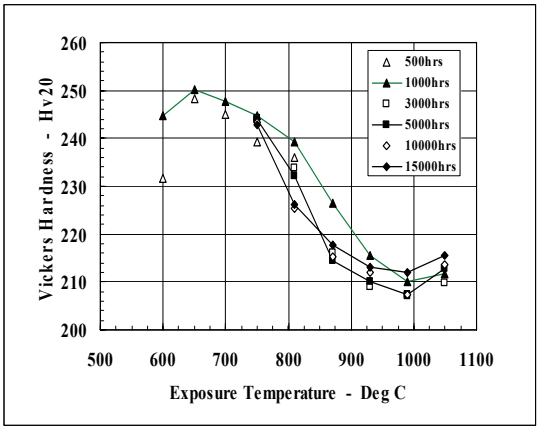

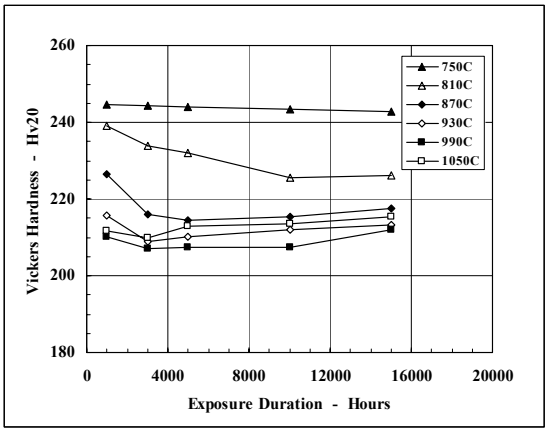

Figures 2a) and b) Variation of hardness with exposure temperatures and times

Examination of the 1000 hours exposure curve indicates that following initial hardening, re-softening of the alloy occurs with increasing exposure temperature with the original hardness level being regained at a temperature of approximately 925°C. Above 925°C further softening occurs with the curve reaching a minimum of ~210Hv20 at about 990°C, before rising at 1050°C. Exposures for longer durations follow similar patterns with the curves for 3, 5 10 and 15 thousand hours being almost superimposed. The data shown in Figure 2a also suggests that in the unstressed condition the maximum degree of thermal hardening occurs between 600°C and 700°C with the maximum softening temperature for the alloy being close to 1000°C.

The hardness data can also be usefully plotted against a time - temperature function such as the Larson-Miller parameter, defined as $P = T(C + \log t)/1000$, where P is the Larson-Miller parameter, T is the exposure temperature in degrees Kelvin, t is the exposure duration in hours and C is the Larson-Miller constant, with a value of 20 often being used for convenience. As is evident from Figure 3a, maximum and minimum hardness values of approximately 250Hv20 and 208Hv20 are observed in the Hv v LMP plot at P-values of approximately 22 and 30 respectively.

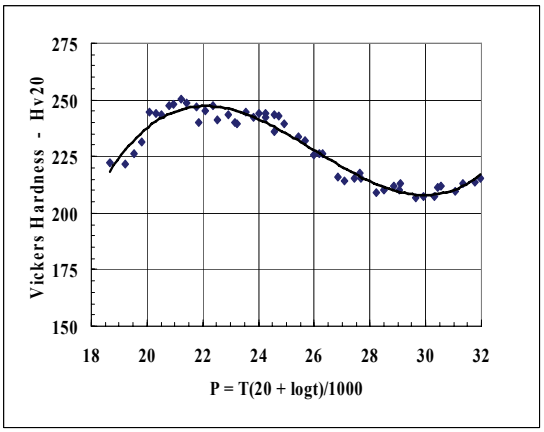

3a) Thermally exposed data up to 15000 hours

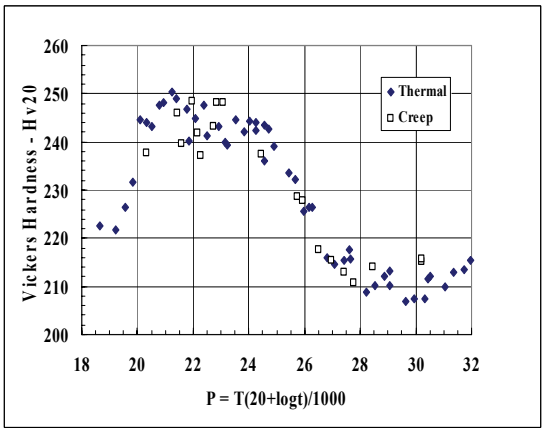

3b) Thermally exposed and creep exposed data

Figures 3a) and b) Hardness data for thermally exposed and creep tested HA230 in the temperature range 600°C-1050°C

A least squares regression analyses of the data shown in Figure 3a indicates that a good fit is obtained using a third degree polynomial of the form,

$$Hv = aP^3 + bP^2 + cP + d$$

where a, b, c and d are constants, Hv is the hardness value and P is the Larson-Miller parameter.

Using a C value of 20 gives the following best fit equation for these data with a R^2 value of 0.9441.

$$Hv = 0.16\,P^3 - 12.59P^2 + 320.28P - 2420$$

Creep Exposure Tests

Vickers hardness measurements on sections from unstressed areas in the heads of the fractured creep rupture test pieces are compared with the thermal exposure hardness data in Figure 3b. Although the data set is smaller, the hardness values lie close to, and follow the same trend as those obtained for the thermally exposed tests. In addition, comparison of the two data sets show that once more the maximum and minimum hardness values occur at Larson-Miller parameter values of approximately 22 and 30 respectively.

Regression analysis of the hardness data from the creep rupture specimen heads also gives a good fit with a third order polynomial in P with a R^2 value of 0.9414 being obtained, Table 4. On the basis of this analysis and the closeness of the match between the hardness data sets shown in Figure 4, it is considered that the data from the thermal and creep exposure tests can reasonably be pooled and the combined data analysed to produce a Master hardness v Larson-Miller parametric plot for this alloy. Regression analysis of the combined data indicates that use of a cubic polynomial to represent the data is once more valid resulting in a R^2 value of 0.9304 with the following master Hardness v Larson-Miller equation representing variations in hardness on unstressed HA230 exposed for durations of up to 15,000 hours at temperatures in the range of 600°C to 1050°C.

$$Hv = 0.16P^3 - 12.46P^2 + 316.17P - 2381.6$$

Exposure	Values of regression constants and R^2				
Data	a	b	c	d	R^2
Thermal Exposure	0.161	-12.59	320.28	-2420.2	0.9441
Creep Heads	0.233	-17.85	448.24	-3455.9	0.9414
Combined Data	0.160	-12.46	316.17	-2381.6	0.9304

Table 4 Regression constants and values for thermally exposed HA230 hardness data

Metallographic Studies

Thermally Exposed HA230

Optical microscopy studies on HA230 coupons thermally exposed for up to 15000 hours at temperatures in the range 750°C to 1050°C have revealed microstructural features which can be directly correlated with the changes in hardness described in Figures 2a and b. For example, following exposure for 1000 hours at 750°C an increase in hardness of 12.3% above that of the as-received material condition is observed due to precipitation of $M_{23}C_6$ type carbides, on the original grain boundaries and annealing twins. Further exposure at this temperature results in gradual softening of the material with hardnesses of 11.9%, 11.7% and 11.4% above that of the as-received condition being recorded for exposure durations of 5000, 10,000 and 15,000 hours. Optical microscopy indicates that this re-softening at 750°C is associated with progressive coarsening of $M_{23}C_6$ type followed by gradual resolution of these precipitates in the microstructure, Figure 4. Similar observations have been reported by Jordan, et al [6] as well as Whittenberger [7] in studies of unstrained HA230 exposed for 10,000 hours at temperatures in the range 750°C to 1050°C.

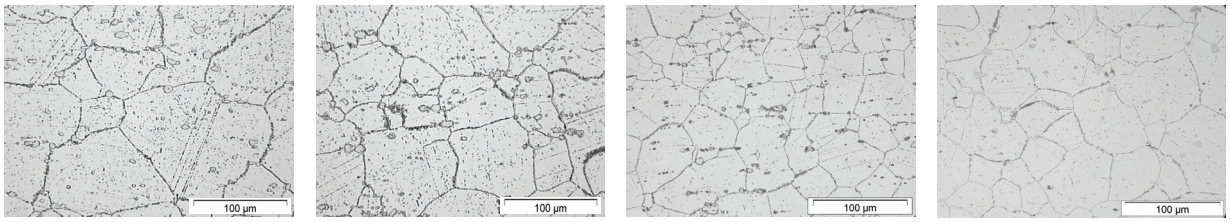

1000 hrs 5000 hrs 10,000 hrs 15,000 hrs

Figure 4 Effect of exposure duration on microstructure of HA230 exposed at 750°C

Exposure for the same durations at the higher temperatures of 810°C, 870°C, 930°C, 990°C and 1050°C results in more rapid re-softening of the material with hardnesses falling below that observed in the as-received condition after about 2000 hours at temperatures above 810°C as shown in Figure 2b.

The overall changes in microstructure due to high temperature thermal exposure are more evident at the longer exposure durations as evident in the micrographs shown in Figures 5a - f. At exposure temperatures of 870°C and 930°C precipitation appears to be more continuous at the grain boundaries. However, at 990°C and 1050°C a radical change is evident with isolated rounded precipitates apparent within the grains and as strings at the grain boundaries, together with other large pool-like phases present in the microstructure.

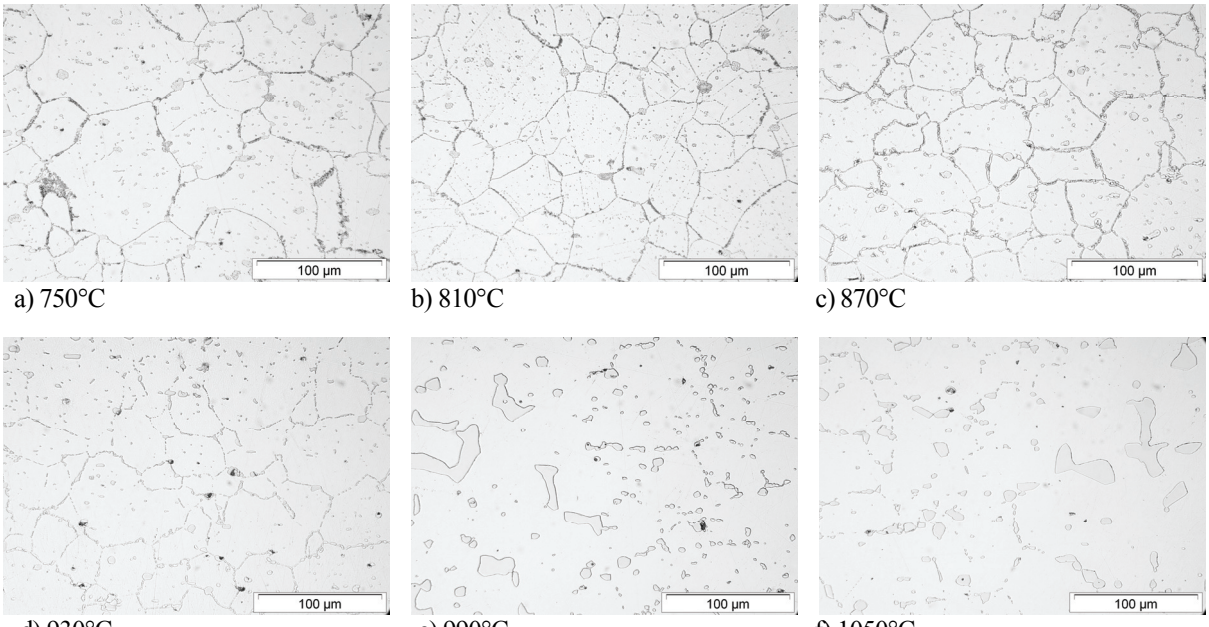

a) 750°C b) 810°C c) 870°C

d) 930°C e) 990°C f) 1050°C

Figure 5 a-f Effects of 15,000 hours exposure at temperatures from 750°C to 1050°C on the microstructure of unstressed HA230

Creep Tested HA230

Optical microscopy studies have also been carried out on microsections taken from the gauge lengths of selected creep rupture specimens, as well as from unstressed areas of the corresponding specimen heads, and the microstructures observed compared with those found in the solution annealed and thermally exposed material described above, Table 5.

Testpiece	Temperature °C	Rupture Life Hours	Elongation %	Larson-Miller Parameter
DKX	650	6577	20.7	21.98
DLA	700	18160	17.2	23.60
DLB	700	4995	-	23.05
DLH	900	28776	~ 35	28.69
COD	950	50874	66.7	30.21
COG	1000	5366	70.8	30.20

Table 5 - Creep rupture test results on HA230

In all instances the fractures were intergranular with the creep damage in the form of cracking and grain boundary voiding being observed all along and normal to the axial load on the test pieces. In DKX, DLA and DLB the creep damage was mainly in the form of transverse intergranular cracks, while in specimens DLH, COD and COG, tested at the higher temperatures the damage was mainly in the form of large voids located on the grain boundaries normal to the applied stress, Figures 6a - f.

The general microstructure observed in gauge length and unstressed head regions of testpieces DKX, DLA and DLB consisted of chromium rich $M_{23}C_6$ type carbides precipitated at the grain boundaries and original annealing twin boundaries, together with large primary M_6C carbides randomly distributed throughout the matrix. However, unlike the thermally exposed material, fine $M_{23}C_6$ precipitates were also found to be present in the creep strained gauge length regions of these test pieces. Both the grain and twin boundary precipitation appeared to be more pronounced in testpieces DLA and DLB compared with that observed in DKX. This may be due to these tests having been carried out at 700°C compared with 650°C in the case of testpiece DKX and further supports the observations already made regarding the effects of temperature on the microstructures of the thermal exposed HA230 specimens.

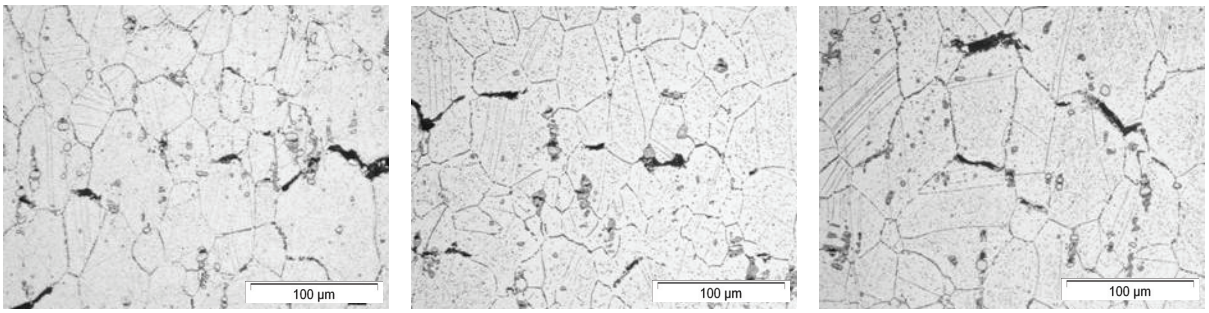

a) DKX - 6577 hrs at 650°C b) DLA - 18160 hrs at 700°C c) DLB - 4995 hrs at 700°C

d) DLH - 28777 hrs at 900°C e) COD - 50874 hrs at 950°C f) COG - 5366 hrs at 1000°C

Figures 6 a - f Microstructures of gauge lengths in HA230 creep rupture test pieces

The microstructures observed in test pieces DLH, COD and COG were totally different from those found in the gauge lengths of DKX, DLA and DLB. In the case of test DLH, which ruptured after 28776 hours at 900°C, the precipitation was almost continuous along the grain boundaries with coarse particles being also randomly present within the grains. Whereas it was possible to differentiate between the primary and grain boundary carbide types in testpieces DKX, DLA and DLB, this was not possible optically in testpiece DLH since the particles were very similar in both size and shape. The microstructural differences were even more pronounced in COG, which had fractured after 5366 hours at 1000°C. In this case the grain boundary precipitation was continuous with no evidence of discrete particles being present. However in COD, which fractured after 50874 hours at 950°C and had an identical LPM value to COG, the precipitation appeared in the form of large almost isolated pools with no obvious grain boundary structure being evident. Furthermore while there were marked similarities between the microstructures in the gauge lengths and unstressed head areas of DKX, DLA and DLB this was not the case for the higher temperature tests DLH, COD and COG. In these latter three tests coarse almost continuous precipitation was observed along the grain boundaries together with clear evidence of primary M_6C particles remaining randomly dispersed throughout the respective matrices, Figures 7a-c. These are similar to the microstructures observed in HA230 samples thermally exposed for 10,000 hours at 930°C and 990°C as shown in Figures 7d and e.

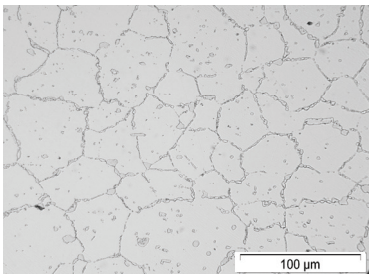

a) DLH - 28777 hrs at 900°C

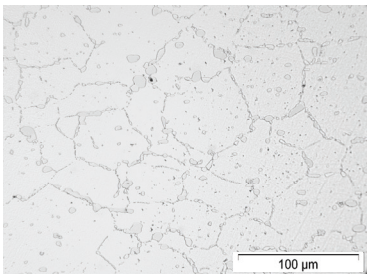

b) COD - 50874 hrs at 950°C

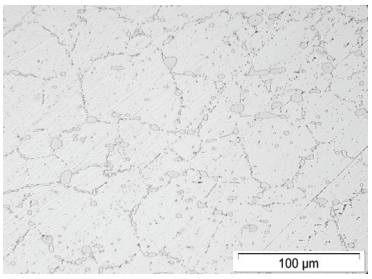

c) COG - 5366 hrs at 1000°C

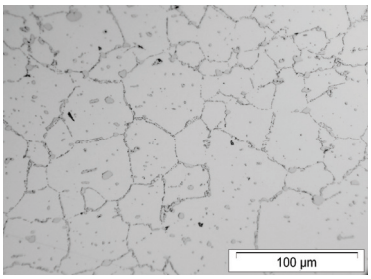

d) 10,000 hrs at 930°C

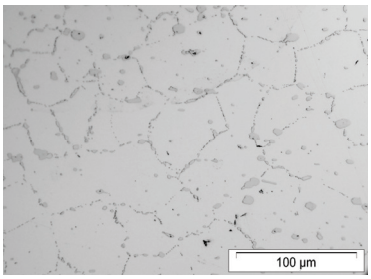

e) 10,000 hrs at 990°C

Figures 7 a-e Comparison of microstructures of unstressed heads of DLH, COD and COG creep tests and thermally exposed HA230

However reverting back to highest temperature creep tests it is interesting to note that whereas the microstructure in the gauge length of DLH is a coarser version of that found in its unstrained head, pool-like precipitates similar to those observed in the gauge lengths of COD and COG have only been observed in material thermally exposed for 15,000 hours at 990°C and 1050°C, Figures 6e and 6f. This suggests that the microstructural evolution observed in the creep tested material also occurs as a result of thermal exposure but at a much slower rate in the absence of plastic deformation due to creep.

FEGSEM Studies

Preliminary FEGSEM studies have confirmed, as shown by Vecchia et al [8], that the phases occurring in thermal and creep exposed HA230 can readily be distinguished by their chemical signatures. Using backscattered electron imaging and EDX mapping, a qualitative assessment can be readily made regarding the distribution of specific phases within the microstructure, while EDX point and line scan analysis techniques enable the compositions of both the matrix and individual phases to be determined quantitatively. For example, FEGSEM images and EDX distribution maps for nickel, chromium and tungsten are shown for a section from the gauge length of creep specimen DLH in Figure 8. These maps clearly show the networks of chromium rich $M_{23}C_6$ grain boundary precipitates, together with large tungsten rich primary M_6C precipitates, in addition to other unidentified tungsten containing particles at the grain boundaries. In addition, EDX point analyses for primary M_6C and grain boundary precipitates, as well as the alloy matrix are also presented in Figure 8. Typical EDX line scans across a primary M_6C precipitate and a two-phase grain boundary particle are shown in Figures 9a and b.

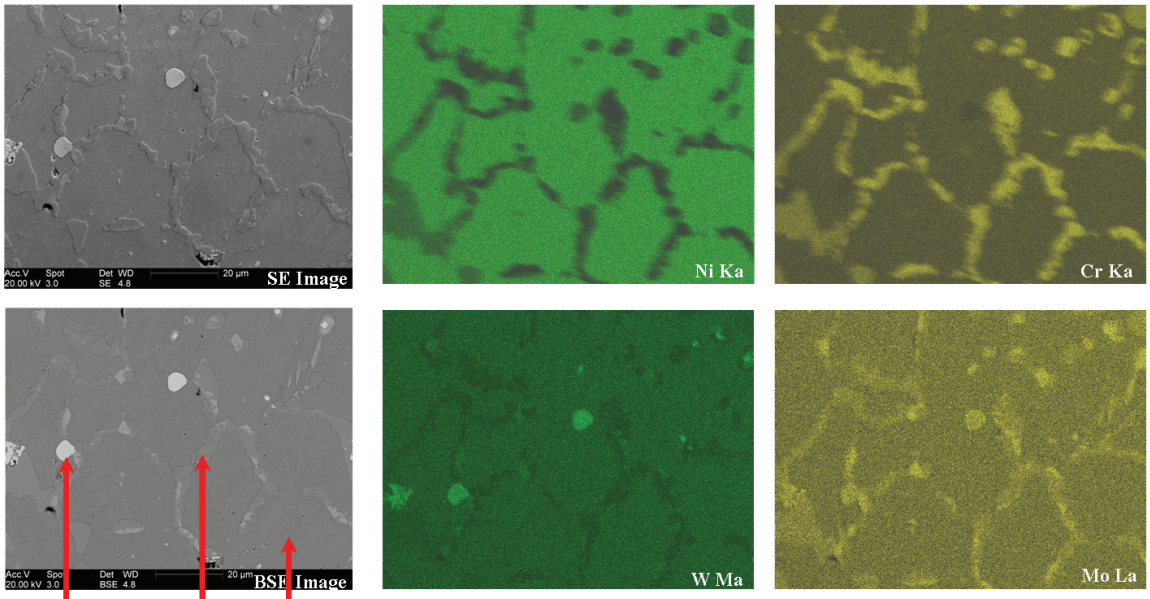

EDX Analyses Of The Different Phases (Wt%)				
	Cr	Mo	W	Ni
Matrix	17.07	2.80	17.23	62.90
$M_{23}C_6$	40.13	4.74	24.44	30.79
M_6C	10.87	5.25	67.87	16.01

Figure 8 EDX analysis of particles and element mapping in gauge length of creep test DLH

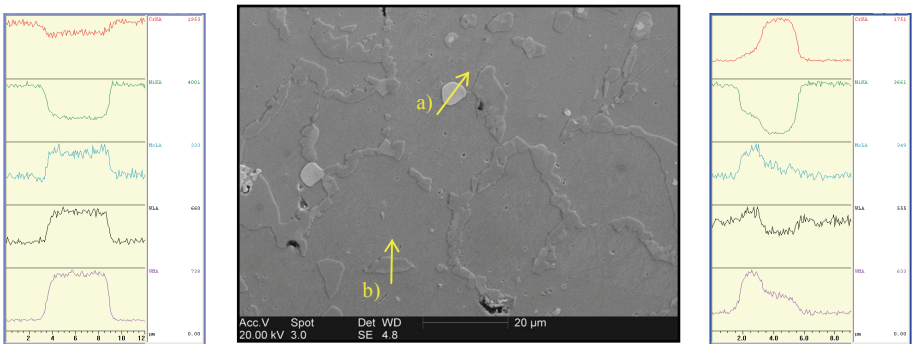

a) Primary M_6C b) Composite gb particle

Figures 9a) and b) EDX Line scans through particles in gauge length of creep test DLH

Similar FEGSEM distribution maps for nickel, chromium, tungsten and molybdenum from the gauge length region of creep specimen COG are shown in Figure 10. These maps clearly show that in this case both grain boundary and individual precipitates in the microstructure are enriched on chromium, tungsten and molybdenum. In addition, EDX point analyses for three forms of precipitates, as well as the alloy matrix, are also presented in Figure 10. EDX line scans across typical precipitates are shown in Figure 11.

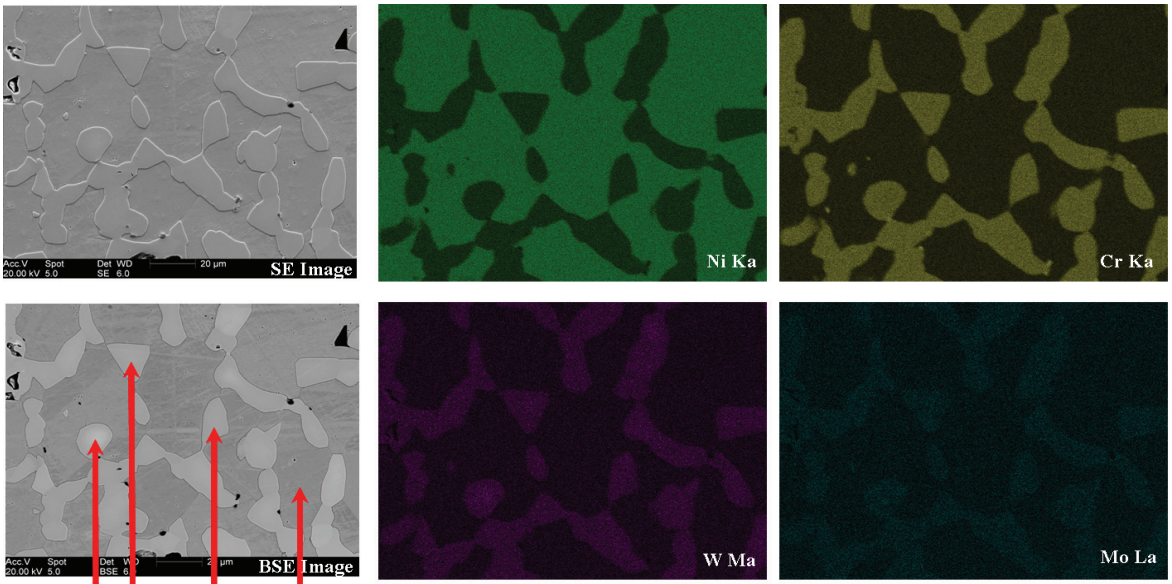

EDX Analyses Of The Different Phases (Wt%)				
	Cr	Mo	W	Ni
Matrix	12.55	2.60	13.36	71.49
Lenticular (L)	13.61	1.51	15.06	69.81
Triangular (T)	40.42	5.24	24.01	30.34
Rounded (R)	34.33	4.08	20.43	41.16

Figure 10 FEGSEM and EDX images of carbides present in gauge length of creep test piece COG

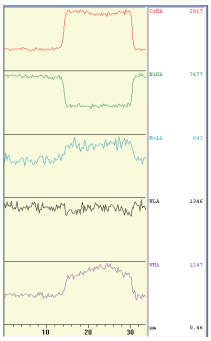

a) Rounded particle

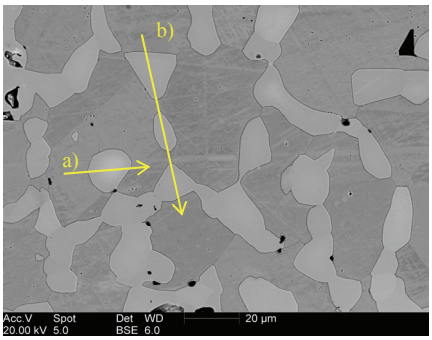

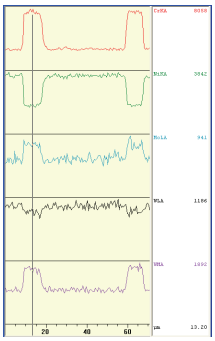

b) Triangular and lenticular particles

Figures 11a) and b) EDX Line scans through particles in gauge length of creep test COG

A comparison of the EDX point analysis data from the gauge lengths of creep specimens DLH and COG shows that there are significant differences between the compositions of both the matrix and the precipitated phases in these samples. For example, preliminary results indicate that while the molybdenum contents of the matrices are similar, there are significant differences in their respective chromium, tungsten and nickel contents. In DHL, both the chromium and tungsten contents are similar at 17.1% and 17.2% respectively, while in COG the corresponding values are 12.5% and 13.3%. These are balanced by changes in the nickel content of the DHL matrix of 62.9% and 71.4 in the matrix of COG. It is also worth noting the differences in the types and composition of precipitates found in the gauge lengths of the DHL and COG creep specimens. In the former both M_6C and $M_{23}C_6$ phases appear to be present with the latter in combination with another unidentified phase at the grain boundaries. In COG the situation differs with clear evidence of rounded, triangular and pool-like precipitation with variable compositions, none of which have so far been identified. No evidence of the primary M_6C precipitate has been observed in the gauge length of this creep specimen.

Conclusions

The results to date have demonstrated that hardness data from thermal and creep exposure tests conducted on HA230 for up to 50,000 hours in the temperature range 600°C to 1050°C can be combined and analysed for the purposes of generating a master Hardness v Larson-Miller parametric plot, which may be used for the purposes of estimating average in-service exposure temperatures for this alloy. A least squares regression analysis has shown that a cubic polynomial between hardness and the Larson-Miller parameter gives a good fit to these data with an R^2 value of 0.9304.

Optical microscopy and FEGSEM studies on thermally exposed HA230 have revealed microstructural factors, which can be correlated with the observed changes in hardness due to thermal exposure over the range of temperature and durations investigated. The results have shown that the initial increases in hardness above that of the alloy in the as-received solution annealed condition are consistent with precipitation of fine $M_{23}C_6$ carbides at grain boundaries and original annealing twin boundaries within the grains. Subsequent exposure for long durations at high temperatures results in re-softening of the alloy. This is considered to be due to progressive $M_{23}C_6$ coarsening and the formation of other phases within the alloy. Current studies are aimed at evaluating the precipitation sequences due to long-term thermal exposure at temperatures up to 1050°C in this alloy.

Similar studies conducted on the heads and gauge length regions of creep tested HA230 have shown that at the lower test temperatures [650°C to 750°C] the microstructures were similar to those observed in the thermally exposed material. However at test temperatures above this an almost continuous precipitation is present at grain boundaries together with coarse particles apparently randomly distributed within the grains. The effect of creep strain on the microstructure was most pronounced at the highest testing temperatures [950°C and 1000°C] where significant changes were apparent in both the appearance and composition of precipitation both in the heads and gauge length regions of the creep test pieces. Once more, changes in the microstructure in the heads of these test pieces was mirrored in the microstructures of the thermally exposed coupons exposed for 15,000 hours at temperatures > 900°C.

Acknowledgements
The authors would like to thank their respective organizations for their support in this work and kind permission to publish this paper. The authors are also grateful to the COST538 consortium for facilitating the programme that this study forms part of.

References

1. HAYNES 230 Alloy Product Brochure, H-3000, Haynes International. www.haynesintl.com

2. D L Klarstrom, The Development of Haynes 230 Alloy, Corrosion 1994, NACE International, pp 407/1 – 407/12

3. D L Klarstrom, Heat treatment/Property Relationships for Solid-Solution Strengthened Heat Resisting Alloys, 1st International Conference on Heat Resistant Materials, Lake Geneva, September 22-26, 1991

4. D L Klarstrom, The Thermal Stability of a Ni-Cr-W-Mo Alloy, NACE Corrosion 94, Paper No. 407, NACE International, Houston, TX, 1994

5. S J Matthews, Thermal Stability of Solid Solution Strengthened High Performance Alloys, Superalloys: Metallurgy and Manufacture, pp 215-226 , Claiter's Publishing, Baton Rouge, LA, 1976

6. C E Jordan, Raserfske, R.K., Castagna, A., Thermal Stability of High Temperature Structural Alloys, *Long Term Stability of High Temperature Materials. Proceedings of Symposium. Held during the 1999 TMS Annual Meeting*, 1999, p 55-67

7. J D Whittenberger, 77 to 1200K Tensile Properties of Several Wrought Superalloys after Long-term 1093K Heat Treatment in Air and Vacuum, Journal of Materials Engineering and Performance, Vol 3(1), Feb 1994, pp91-103

8. K S Vecchio, Fitzpatrick, M. D., Klarstrom, D., Influence of subsolvus thermomechanical processing on the low-cycle fatigue properties of HAYNES 230 alloy, Met and Matls Trans A, Vol26A, n 3, Mar, 1995, pp 673-689